Supplementary Information

Microkinetic Simulations of Ketene Conversion to Olefins in H-SAPO-34 Zeolite for Bifunctional Catalysis

Jun Ke, Yang-Dong Wang, Chuan-Ming Wang*, Zai-Ku Xie*

State Key Laboratory of Green Chemical Engineering and Industrial Catalysis, Sinopec Shanghai Research Institute of Petrochemical Technology Co. Ltd., Shanghai 201208, China

*E-Mail: wangcm.sshy@sinopec.com; xzk@sinopec.com

Table S1. Reaction energies (ΔE) and energy barriers (E_a) at 0 K, forward rate constants (k_{fwd}) and backward rate constants (k_{bkd}) at 673 K of the involved elementary steps for the conversion of ketene to olefins in H-SAPO-34.

	Elementary step	ΔE / eV	E_a / eV	k_{fwd} / s^{-1}	k_{bkw} / s^{-1}
R1	$CH_2CO \cdot HZ = CH_3COZ$	−0.42	0.03	2.4×10^{11}	6.4×10^{9}
R2	$C_2H_4 \cdot CH_3COZ = CO \cdot$ 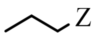	0.06	2.01	3.2×10^{-2}	8.8×10^{-1}
R3	$C_3H_6 \cdot CH_3COZ = CO \cdot$ 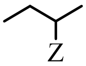	0.18	1.86	1.5×10^{-1}	4.4×10^{2}
R4	$C_3H_6 \cdot CH_3COZ = CO \cdot$ 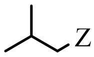	0.43	1.86	1.5×10^{-1}	2.9×10^{4}
R5	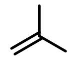 $\cdot CH_3COZ = CO \cdot$ 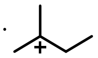 $\cdot Z^-$	0.58	1.72	2.3×10^{1}	8.2×10^{2}
R6	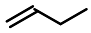 $\cdot CH_3COZ = CO \cdot$ 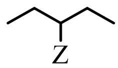	0.22	1.82	1.1×10^{0}	3.9×10^{3}
R7	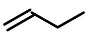 $\cdot CH_3COZ = CO \cdot$ 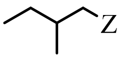	0.45	1.82	1.1×10^{0}	5.9×10^{4}
R8	 $\cdot CH_3COZ = CO \cdot$ 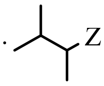	0.69	1.68	1.4×10^{1}	3.0×10^{5}
R9	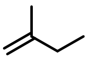 $\cdot CH_3COZ = CO \cdot$ 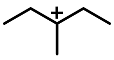 $\cdot Z^-$	0.44	1.62	2.1×10^{1}	8.8×10^{1}
R10	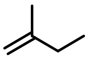 $\cdot CH_3COZ = CO \cdot$ 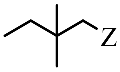	0.60	1.62	2.1×10^{1}	1.2×10^{7}
R11	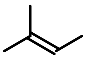 $\cdot CH_3COZ = CO \cdot$ 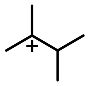 $\cdot Z^-$	0.56	1.62	1.3×10^{1}	1.4×10^{3}
R12	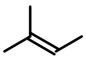 $\cdot CH_3COZ = CO \cdot$ 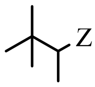	0.95	1.62	1.3×10^{1}	7.2×10^{5}
R13	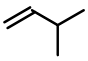 $\cdot CH_3COZ = CO \cdot$ 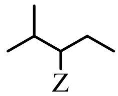	0.66	1.78	1.8×10^{0}	1.7×10^{4}
R14	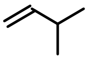 $\cdot CH_3COZ = CO \cdot$ 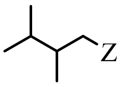	0.69	1.78	1.8×10^{0}	7.6×10^{6}
R15	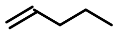 $\cdot CH_3COZ = CO \cdot$ 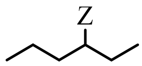	0.27	1.81	3.1×10^{-1}	1.3×10^{4}
R16	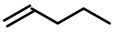 $\cdot CH_3COZ = CO \cdot$ 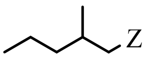	0.43	1.81	3.1×10^{-1}	7.3×10^{4}
R17	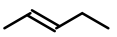 $\cdot CH_3COZ = CO \cdot$ 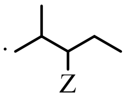	0.81	1.74	2.3×10^{-1}	2.6×10^{5}
R18	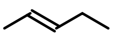 $\cdot CH_3COZ = CO \cdot$ 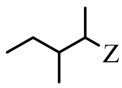	0.86	1.74	2.3×10^{-1}	1.8×10^{6}
R19	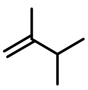 $\cdot CH_3COZ = CO \cdot$ 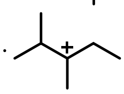 $\cdot Z^-$	0.37	1.69	4.6×10^{0}	3.0×10^{1}
R20	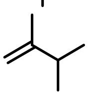 $\cdot CH_3COZ = CO \cdot$ 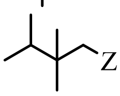	0.63	1.69	4.6×10^{0}	5.1×10^{6}
R21	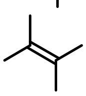 $\cdot CH_3COZ = CO \cdot$ 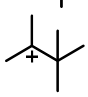 $\cdot Z^-$	0.52	1.55	1.8×10^{2}	2.2×10^{5}
R22	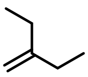 $\cdot CH_3COZ = CO \cdot$ 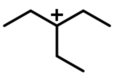 $\cdot Z^-$	0.49	1.70	1.2×10^{1}	3.3×10^{1}

Table S1 (Continued).

	Elementary step	ΔE / eV	E_a / eV	k_{fwd} / s^{-1}	k_{bkw} / s^{-1}
R23	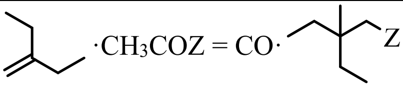 ·CH_3COZ = CO·	0.74	1.70	1.2×10^{1}	1.2×10^{7}
R24	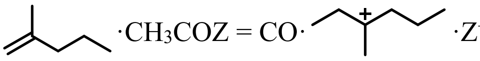 ·CH_3COZ = CO· ·Z^-	0.60	1.74	7.6×10^{-1}	5.4×10^{2}
R25	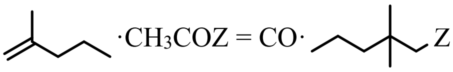 ·CH_3COZ = CO·	0.58	1.74	7.6×10^{-1}	3.5×10^{5}
R26	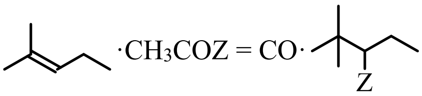 ·CH_3COZ = CO·	0.88	1.57	2.3×10^{1}	4.4×10^{4}
R27	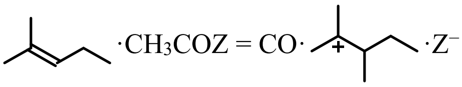 ·CH_3COZ = CO· ·Z^-	0.50	1.57	2.3×10^{1}	3.2×10^{3}
R28	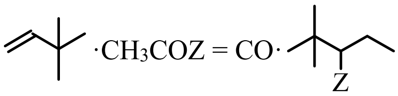 ·CH_3COZ = CO·	0.72	1.77	6.2×10^{-1}	1.7×10^{1}
R29	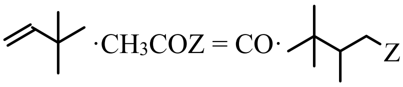 ·CH_3COZ = CO·	0.44	1.77	6.2×10^{-1}	2.4×10^{4}
R30	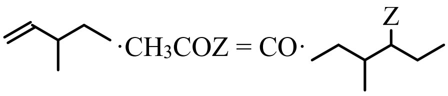 ·CH_3COZ = CO·	0.73	1.81	1.1×10^{0}	3.9×10^{3}
R31	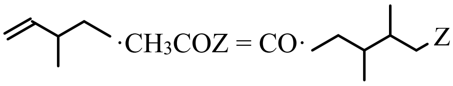 ·CH_3COZ = CO·	0.68	1.81	1.1×10^{0}	4.3×10^{5}
R32	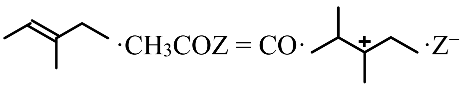 ·CH_3COZ = CO· ·Z^-	0.46	1.60	2.7×10^{1}	9.4×10^{2}
R33	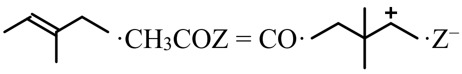 ·CH_3COZ = CO· ·Z^-	1.02	1.60	2.7×10^{1}	2.4×10^{5}
R34	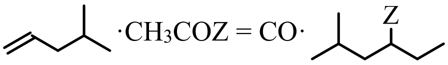 ·CH_3COZ = CO·	0.45	1.84	2.6×10^{-1}	9.1×10^{3}
R35	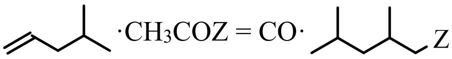 ·CH_3COZ = CO·	0.35	1.84	2.6×10^{-1}	3.6×10^{3}
R36	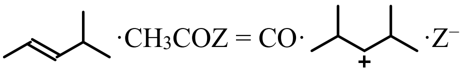 ·CH_3COZ = CO· ·Z^-	0.85	1.75	4.5×10^{0}	1.6×10^{5}
R37	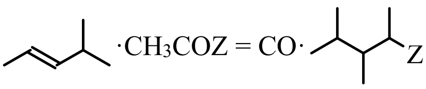 ·CH_3COZ = CO·	1.03	1.75	4.5×10^{0}	4.3×10^{6}
R38	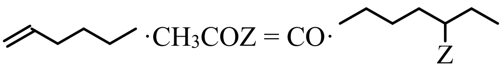 ·CH_3COZ = CO·	0.14	1.76	2.0×10^{0}	7.8×10^{1}
R39	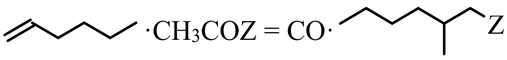 ·CH_3COZ = CO·	0.44	1.76	2.0×10^{0}	1.3×10^{4}
R40	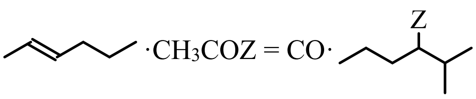 ·CH_3COZ = CO·	0.79	1.70	3.6×10^{0}	3.2×10^{7}
R41	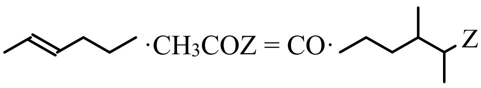 ·CH_3COZ = CO·	0.89	1.70	3.6×10^{0}	1.5×10^{6}
R42	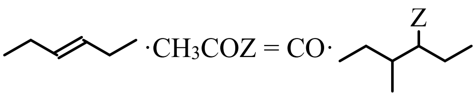 ·CH_3COZ = CO·	0.84	1.76	5.6×10^{0}	8.9×10^{4}
R43	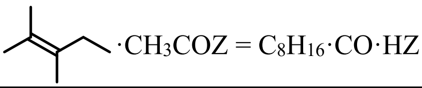 ·CH_3COZ = C_8H_{16}·CO·HZ	−0.03	1.55	1.6×10^{2}	5.7×10^{0}

Table S1 (Continued).

	Elementary step	ΔE / eV	E_a / eV	k_{fwd} / s^{-1}	k_{bkw} / s^{-1}
R44	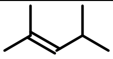 $\cdot CH_3COZ = C_8H_{16}\cdot CO\cdot HZ$	0.05	1.64	1.7×10^{0}	5.6×10^{-1}
R45	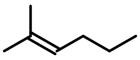 $\cdot CH_3COZ = C_8H_{16}\cdot CO\cdot HZ$	−0.20	1.36	6.1×10^{3}	3.0×10^{0}
R46	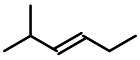 $\cdot CH_3COZ = C_8H_{16}\cdot CO\cdot HZ$	−0.13	1.77	6.5×10^{-1}	2.5×10^{-3}
R47	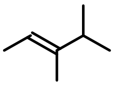 $\cdot CH_3COZ = C_8H_{16}\cdot CO\cdot HZ$	−0.07	1.62	7.4×10^{0}	3.2×10^{-1}
R48	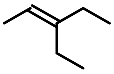 $\cdot CH_3COZ = C_8H_{16}\cdot CO\cdot HZ$	−0.13	1.66	1.6×10^{1}	1.6×10^{-2}
R49	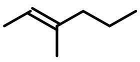 $\cdot CH_3COZ = C_8H_{16}\cdot CO\cdot HZ$	−0.27	1.44	1.5×10^{3}	4.1×10^{-1}
R50	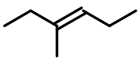 $\cdot CH_3COZ = C_8H_{16}\cdot CO\cdot HZ$	−0.11	1.60	2.3×10^{1}	1.9×10^{-1}
R51	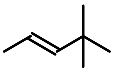 $\cdot CH_3COZ = C_8H_{16}\cdot CO\cdot HZ$	−0.03	1.74	2.4×10^{0}	2.0×10^{-2}
R52	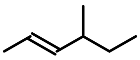 $\cdot CH_3COZ = C_8H_{16}\cdot CO\cdot HZ$	−0.17	1.68	8.2×10^{0}	3.0×10^{-2}
R53	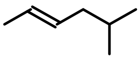 $\cdot CH_3COZ = C_8H_{16}\cdot CO\cdot HZ$	−0.15	1.65	1.0×10^{1}	4.5×10^{-2}
R54	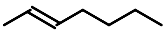 $\cdot CH_3COZ = C_8H_{16}\cdot CO\cdot HZ$	−0.21	1.73	3.7×10^{-1}	2.1×10^{-3}
R55	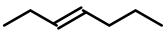 $\cdot CH_3COZ = C_8H_{16}\cdot CO\cdot HZ$	−0.21	1.70	1.8×10^{1}	2.7×10^{-2}
R56	$C_8H_{16}\cdot CH_3COZ = C_9H_{18}\cdot CO\cdot HZ$	0.08	1.57	9.8×10^{0}	1.6×10^{1}
R57	$CH_3COZ = CO\cdot CH_3Z$	0.56	1.96	5.8×10^{-1}	1.7×10^{0}

Table S2. Adsorption energies (E_{ads}) at 0 K of the involved reactant (ketene) and products (CO and light olefins) in H-SAPO-34.

Molecule	E_{ads} / eV	Molecule	E_{ads} / eV
ketene	−0.47	1-butene	−0.71
CO	−0.32	2-butene	−0.68
ethene	−0.42	isobutene	−0.69
propene	−0.57		

Table S3. TS formation energies (E_f) at 0 K of the methylation steps for the conversion of ketene to olefins in H-SAPO-34. The transition states of the stepwise methylation are same to those in the conversion of methanol to olefins [Ref. S1].

	Olefin precursor	E_f / eV Concerted	E_f / eV Stepwise	C_n	Olefin precursor	E_f / eV Concerted	E_f / eV Stepwise
C_2	C_2H_4	0.52	0.56	C_6	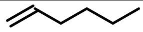	−2.31	−2.17
C_3	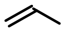	−0.42	−0.35	C_7	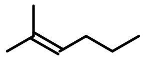	−3.52	−3.23
C_4	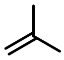	−1.38	−1.28		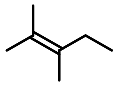	−3.50	−3.40
		−1.30	−1.15		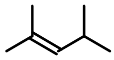	−3.50	−3.37
	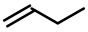	−1.08	−0.93		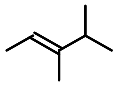	−3.40	−3.25
C_5	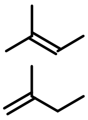	−2.16	−2.01		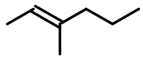	−3.38	−3.17
		−2.00	−1.88		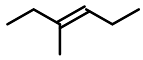	−3.37	−3.29
	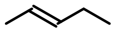	−1.96	−1.85		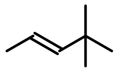	−3.32	−3.16
	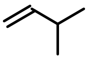	−1.78	−1.65		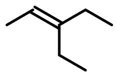	−3.30	−3.23
	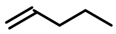	−1.76	−1.60		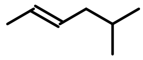	−3.28	−3.03
C_6	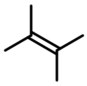	−2.88	−2.73		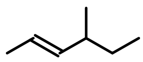	−3.24	−3.05
	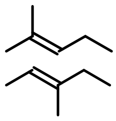	−2.83	−2.71		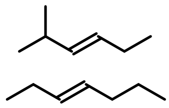	−3.18	−3.08
		−2.78	−2.50			−3.18	−3.01
	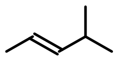	−2.63	−2.51		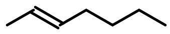	−3.15	−2.95
	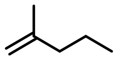	−2.62	−2.43	C_8	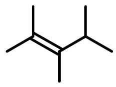	−4.09	−3.96
	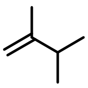	−2.60	−2.51		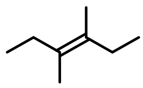	−4.05	−3.97
	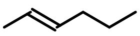	−2.59	−2.36		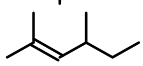	−4.05	−3.86
		−2.55	−2.47		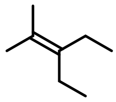	−4.02	−3.97
	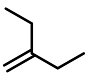	−2.51	−2.47		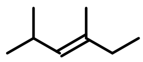	−4.02	−3.92
	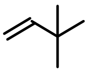	−2.47	−2.22		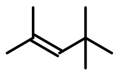	−3.99	−3.86
	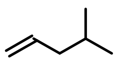	−2.41	−2.22		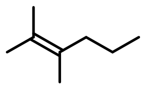	−3.93	−3.86
	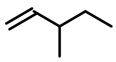	−2.39	−2.18				

Table S4. Elementary steps for the microkinetic simulations of the conversion of ketene to olefins in H-SAPO-34.

$CH_2CO(g) + T = CH_2CO{\cdot}T$	(Eq. S1)
$CO(g) + T = CO{\cdot}T$	(Eq. S2)
$C_nH_{2n}(g) + T = C_nH_{2n}{\cdot}T$ (n = 2–4)	(Eq. S3)
$CH_2CO{\cdot}T + HB = CH_2CO{\cdot}HB + T$	(Eq. S4)
$CO{\cdot}T + HB = CO{\cdot}HB + T$	(Eq. S5)
$CH_2CO{\cdot}HB = CH_3COB$	(Eq. S6)
$CH_3COB = CO{\cdot}CH_3B$	(Eq. S7)
$CO{\cdot}CH_3B + T = CH_3B + CO{\cdot}T$	(Eq. S8)
$CO{\cdot}CH_3B + HB = CH_3B + CO{\cdot}HB$	(Eq. S9)
$C_nH_{2n}{\cdot}HP + CH_2CO{\cdot}T = C_nH_{2n}{\cdot}CH_2CO{\cdot}HP + T$	(Eq. S10)
$C_nH_{2n}{\cdot}HP + CH_2CO{\cdot}HB = C_nH_{2n}{\cdot}CH_2CO{\cdot}HP + HB$	(Eq. S11)
$C_nH_{2n}{\cdot}CH_2CO{\cdot}HP = C_nH_{2n}{\cdot}CH_3COP$	(Eq. S12)
$C_nH_{2n}{\cdot}CH_3COP = CO{\cdot}C_{n+1}H_{2n+3}P$	(Eq. S13)
$CO{\cdot}C_{n+1}H_{2n+3}P + T = C_{n+1}H_{2n+3}P + CO{\cdot}T$	(Eq. S14)
$CO{\cdot}C_{n+1}H_{2n+3}P + HB = C_{n+1}H_{2n+3}P + CO{\cdot}HB$	(Eq. S15)
$C_nH_{2n}{\cdot}CH_3COP = C_nH_{2n}{\cdot}CO{\cdot}CH_3P$	(Eq. S16)
$C_nH_{2n}{\cdot}CO{\cdot}CH_3P + T = C_nH_{2n}{\cdot}CH_3P + CO{\cdot}T$	(Eq. S17)
$C_nH_{2n}{\cdot}CO{\cdot}CH_3P + HB = C_nH_{2n}{\cdot}CH_3P + CO{\cdot}HB$	(Eq. S18)
$C_nH_{2n}{\cdot}HP + CH_3B = HB + C_nH_{2n}{\cdot}CH_3P$ (n = 2–4)	(Eq. S19)
$C_nH_{2n}{\cdot}CH_3P = C_{n+1}H_{2n+3}P$	(Eq. S20)
$C_nH_{2n+1}P = C_nH_{2n+1}P$ (isomerization)	(Eq. S21)
$C_nH_{2n+1}P = C_nH_{2n}{\cdot}HP$	(Eq. S22)
$C_{m+n}H_{2m+2n+1}P = C_mH_{2m}{\cdot}C_nH_{2n}{\cdot}HP$	(Eq. S23)
$C_{m+n}H_{2m+2n+1}P = C_mH_{2m}{\cdot}C_nH_{2n+1}P$	(Eq. S24)
$C_mH_{2m}{\cdot}C_nH_{2n+1}P = C_mH_{2m}{\cdot}C_nH_{2n}{\cdot}HP$	(Eq. S25)
$C_mH_{2m}{\cdot}C_nH_{2n}{\cdot}HP + T = C_mH_{2m}{\cdot}HP + C_nH_{2n}{\cdot}T$ (n = 2–4)	(Eq. S26)
$C_mH_{2m}{\cdot}C_nH_{2n}{\cdot}HP + T = C_nH_{2n}{\cdot}HP + C_mH_{2m}{\cdot}T$ (m = 2–4)	(Eq. S27)
$C_mH_{2m}{\cdot}C_nH_{2n+1}P + T = C_nH_{2n+1}P + C_mH_{2m}{\cdot}T$ (m = 2–4)	(Eq. S28)
$C_mH_{2m}{\cdot}HP + C_nH_{2n}{\cdot}T = C_nH_{2n}{\cdot}HP + C_mH_{2m}{\cdot}T$ (m, n = 2–4)	(Eq. S29)

Table S5. Simulated distribution and evolution rate of each olefinic HCP in H-SAPO-34 for the conversion of ketene to olefins at 673 K and 0.1 MPa. The specific rate of each HCP is normalized to its amount.

Olefinic HCP	Distribution	Specific rate / $s^{-1}\cdot molecule^{-1}$			
		Methylation	Cracking to C_2H_4	Cracking to C_3H_6	Cracking to C_4H_8
C_2	0.54	4.2×10^{-3}	/	/	/
C_3	0.36	0.15	/	/	/
C_4	8.2×10^{-2}	0.72	3.3×10^{-3}	/	/
C_5	1.1×10^{-2}	2.7	3.1	3.1	/
C_6	1.4×10^{-3}	4.7	1.2	15	1.2
C_7	1.4×10^{-7}	0.29	21	4.5×10^{4}	4.5×10^{4}

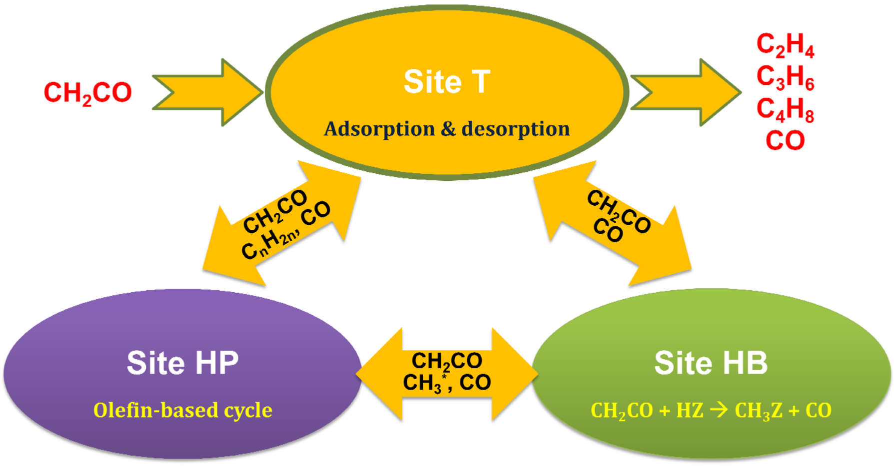

Scheme S1. Proposed three-site model for the microkinetic simulations of the conversion of ketene to olefins in zeolite. Similar model was established previously for the microkinetic simulations of the conversion of methanol to olefins in zeolite [Ref. S1].

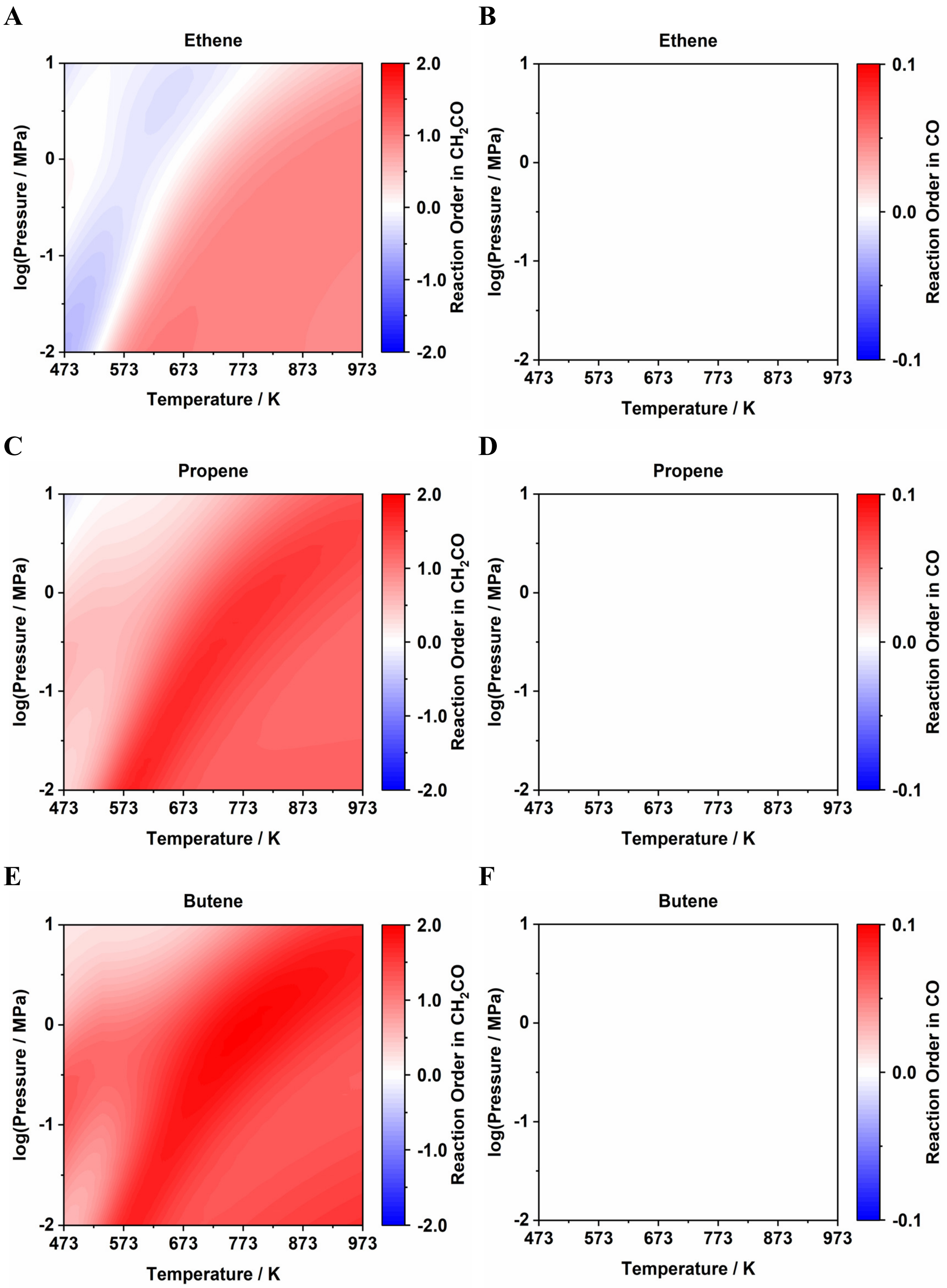

Figure S1. Reaction orders of ethene (**A**, **B**), propene (**C**, **D**), and butene (**E**, **F**) formation in ketene (**A**, **C**, **E**) and CO (**B**, **D**, **F**) as a function of temperature and pressure in H-SAPO-34 for the conversion of ketene to olefins. The default simulation conditions are CH_2CO:CO = 1:1 and HP:HB:T = 1:1:1.

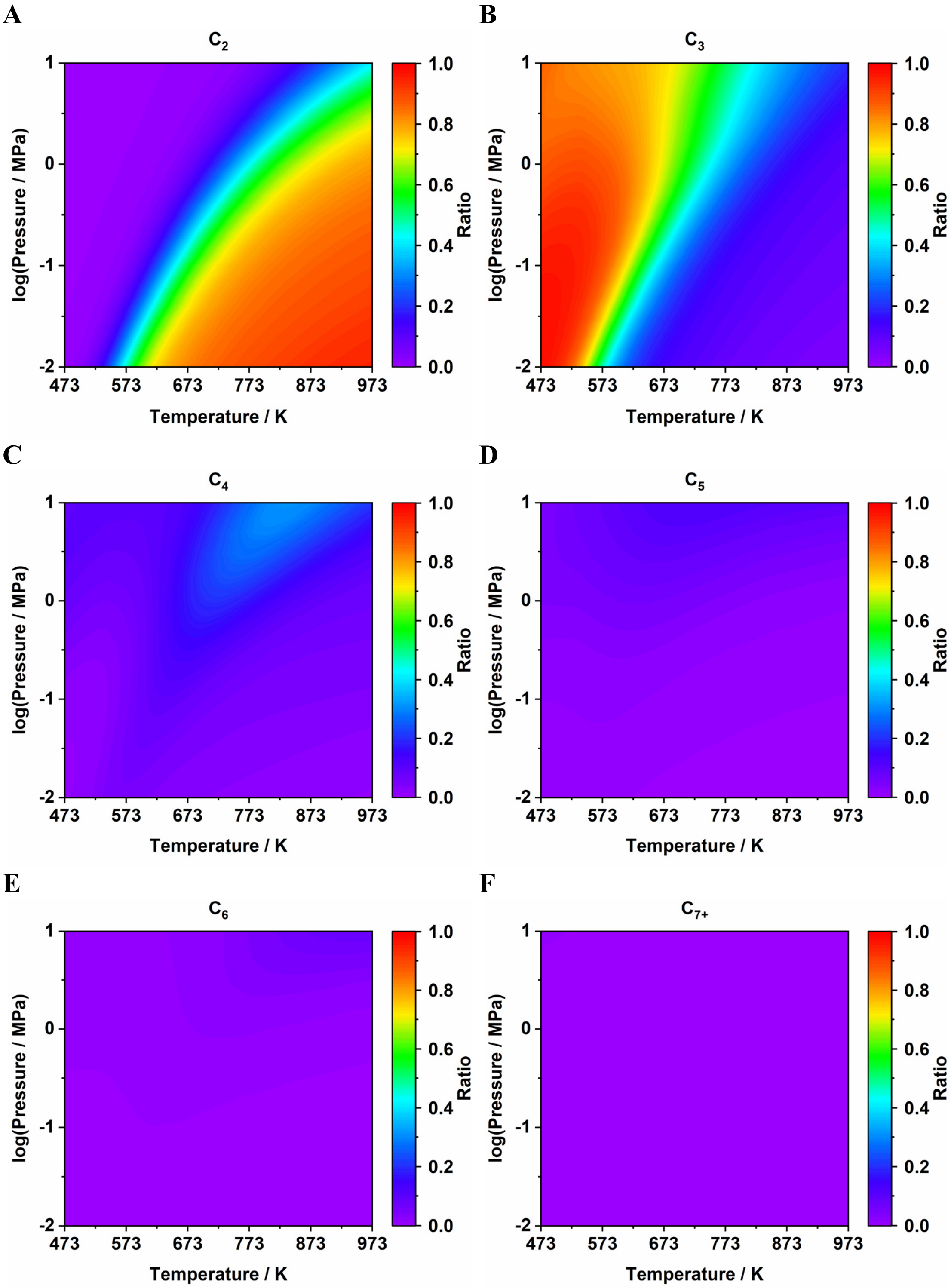

Figure S2. Relative distribution of C_2 **(A)**, C_3 **(B)**, C_4 **(C)**, C_5 **(D)**, C_6 **(E)**, and C_{7+} **(F)** intermediates as a function of temperature and pressure in H-SAPO-34 for the conversion of ketene to olefins.

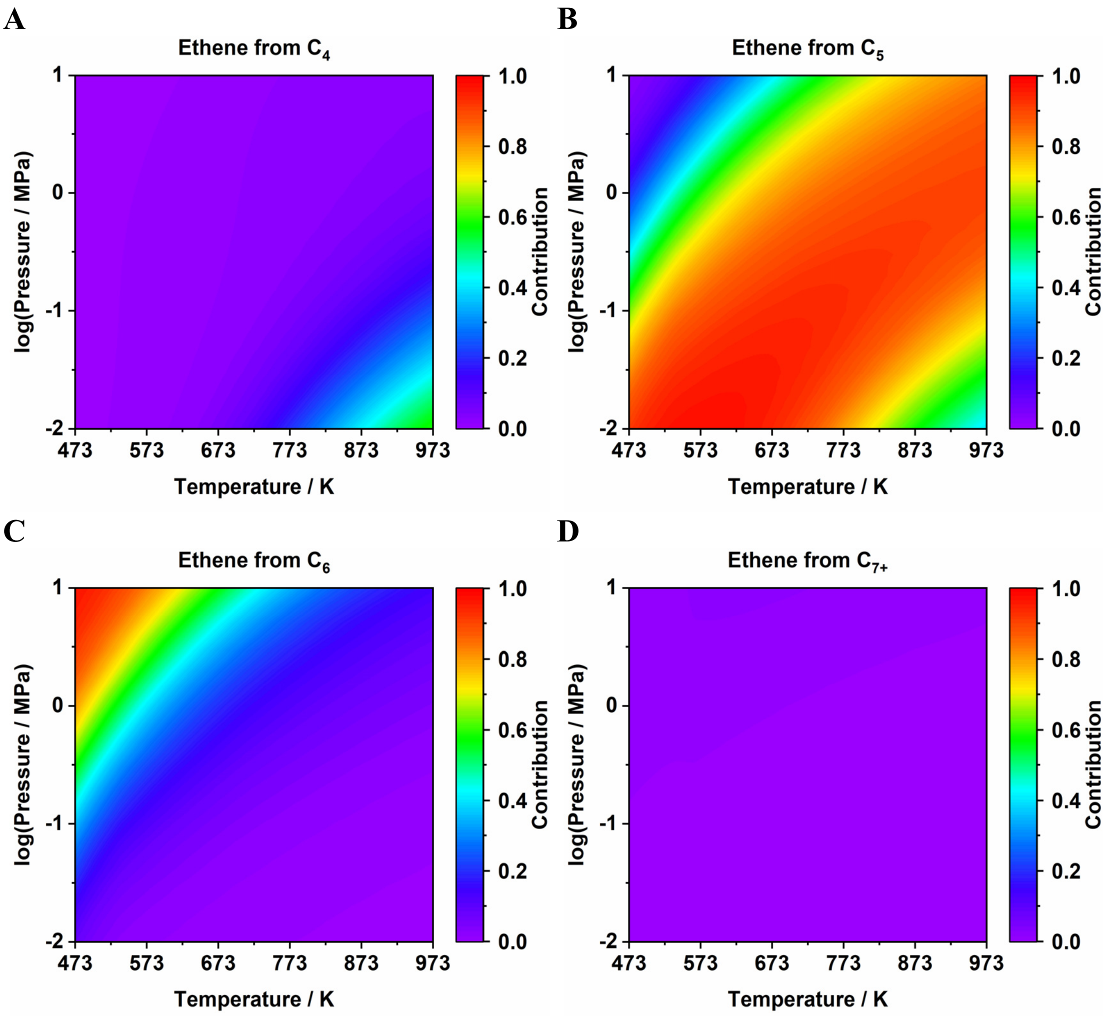

Figure S3. Relative contribution of C_4 **(A)**, C_5 **(B)**, C_6 **(C)**, and C_{7+} **(D)** cracking to produce ethene as a function of temperature and pressure in H-SAPO-34 for the conversion of ketene to olefins.

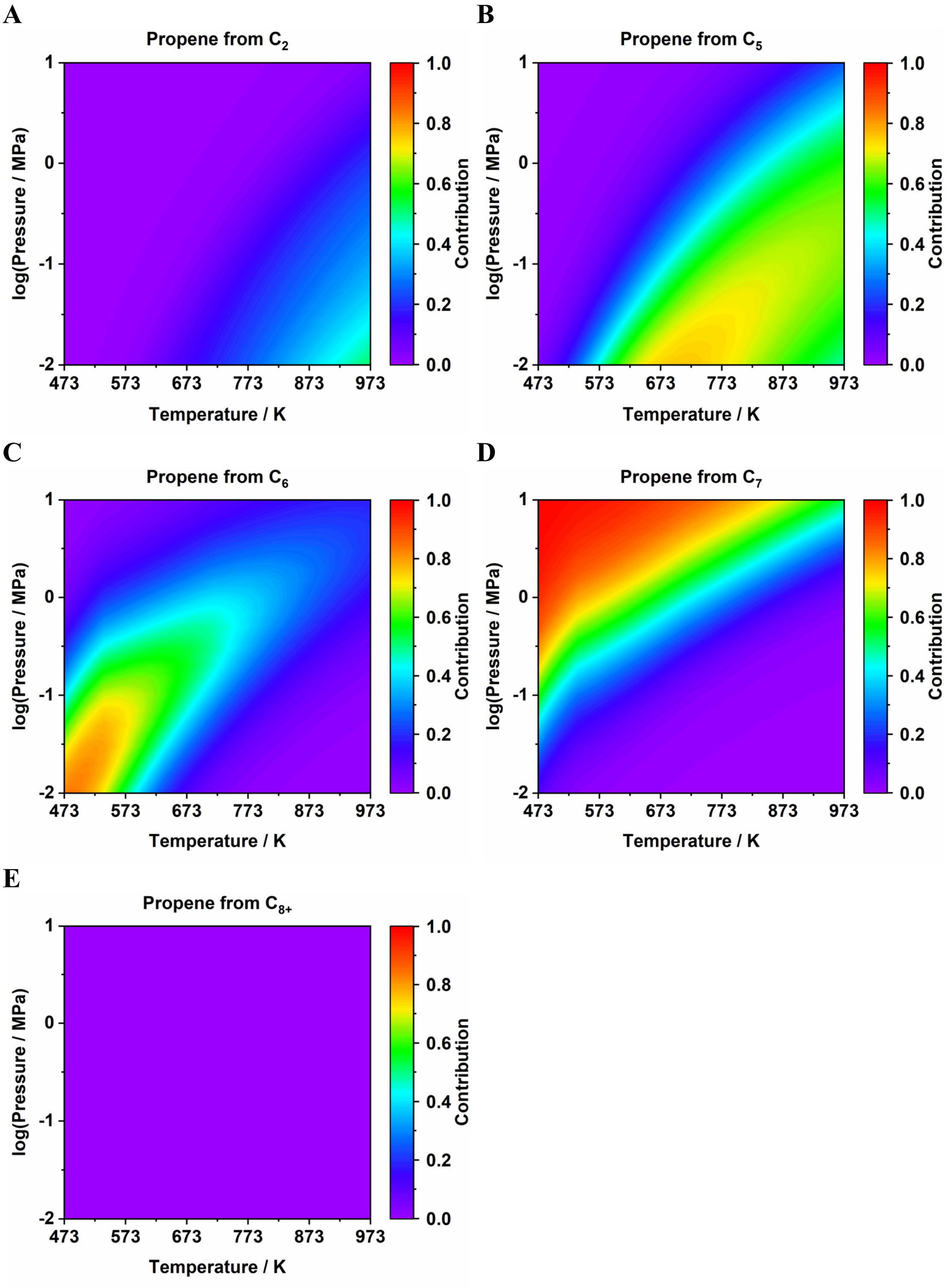

Figure S4. Relative contribution of C_2 methylation **(A)** and C_5 **(B)**, C_6 **(C)**, C_7 **(D)**, and C_{8+} **(E)** cracking to produce propene as a function of temperature and pressure in H-SAPO-34 for the conversion of ketene to olefins.

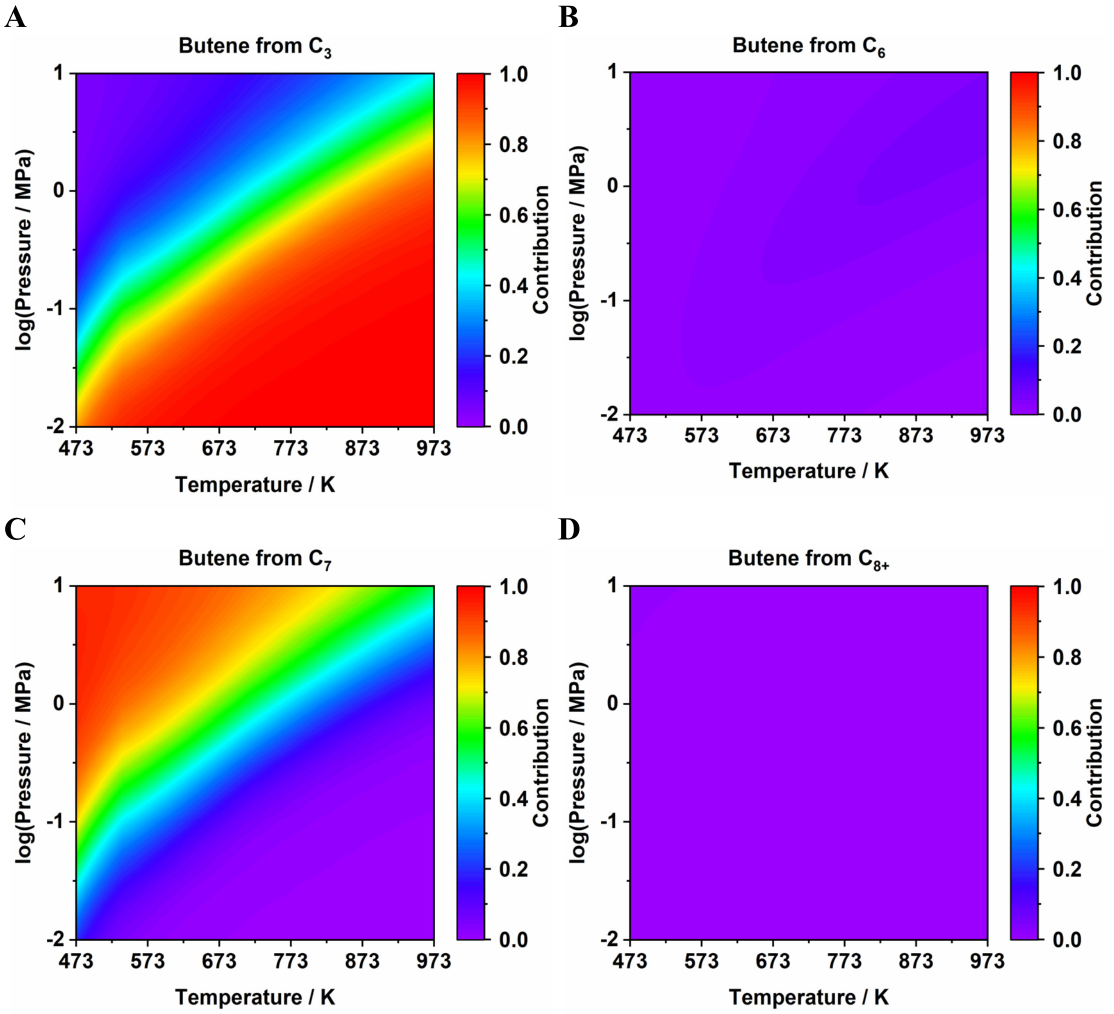

Figure S5. Relative contribution of C_3 methylation **(A)** and C_6 **(B)**, C_7 **(C)**, and C_{8+} **(D)** cracking to produce butene as a function of temperature and pressure in H-SAPO-34 for the conversion of ketene to olefins.

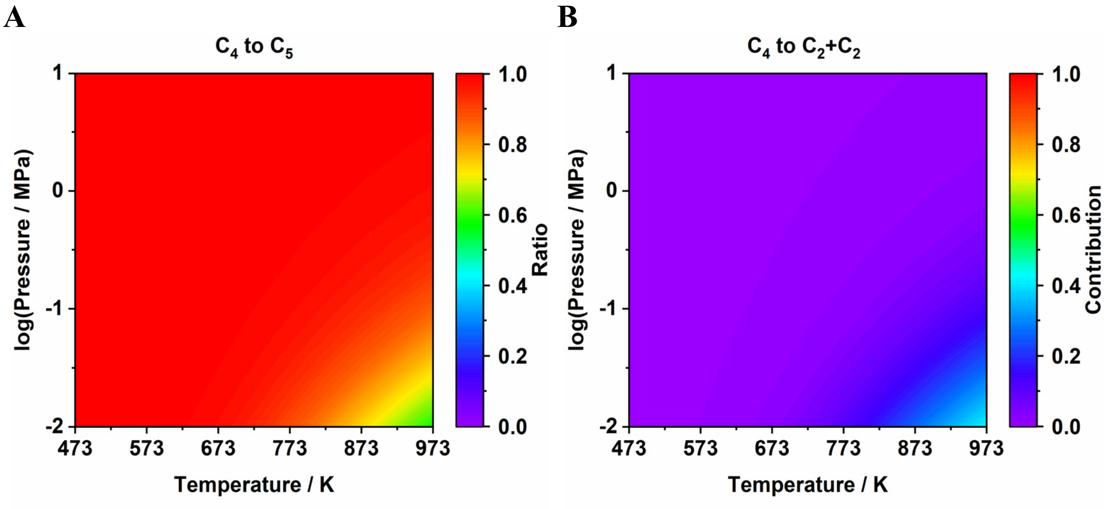

Figure S6. Evolution of C_4 methylation to C_5 **(A)** and C_4 cracking to two C_2 intermediates **(B)** as a function of temperature and pressure in H-SAPO-34 for the conversion of ketene to olefins.

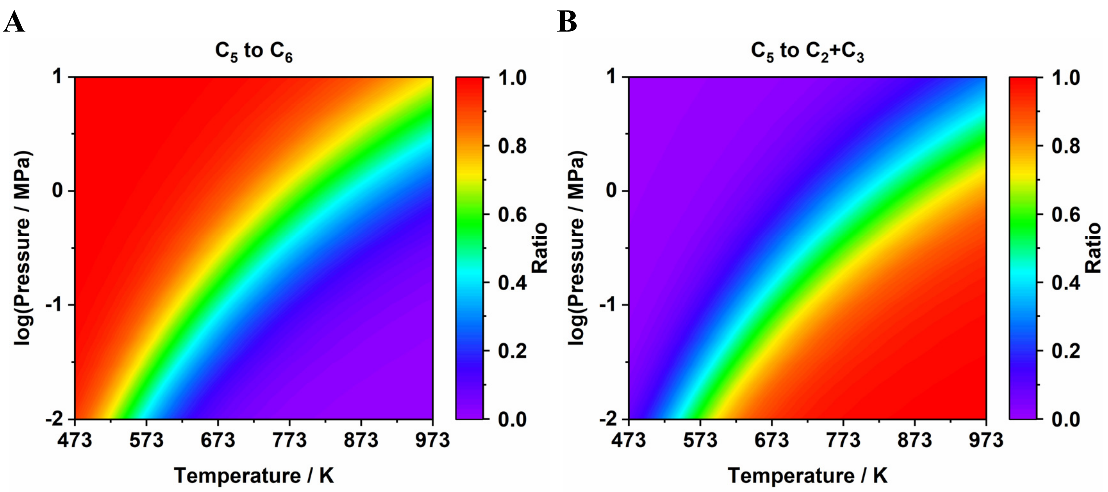

Figure S7. Evolution of C_5 methylation to C_6 **(A)** and C_5 cracking to C_2+C_3 intermediates **(B)** as a function of temperature and pressure in H-SAPO-34 for the conversion of ketene to olefins.

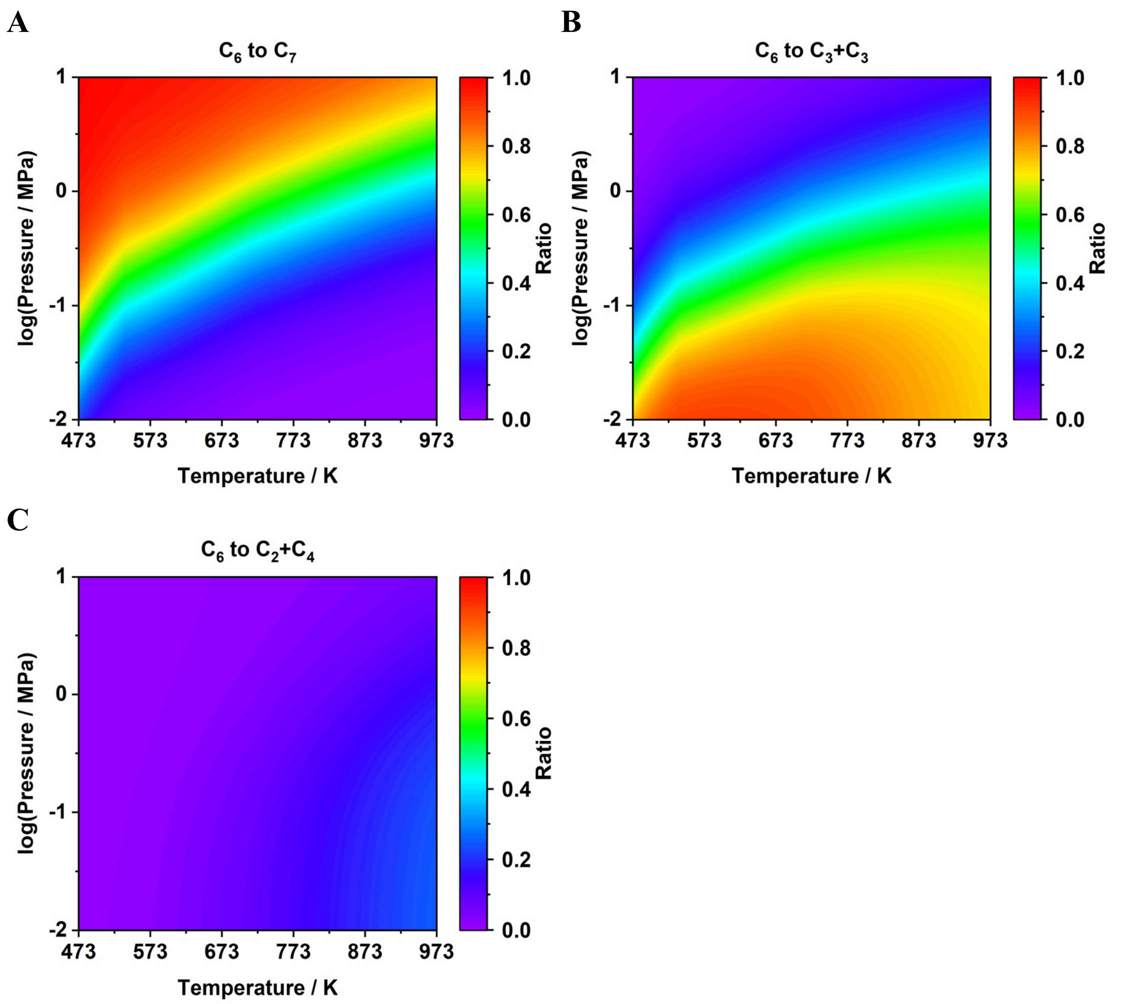

Figure S8. Evolution of C_6 methylation to C_7 **(A)** and C_6 cracking to C_3+C_3 **(B)** and C_2+C_4 **(C)** intermediates as a function of temperature and pressure in H-SAPO-34 for the conversion of ketene to olefins.

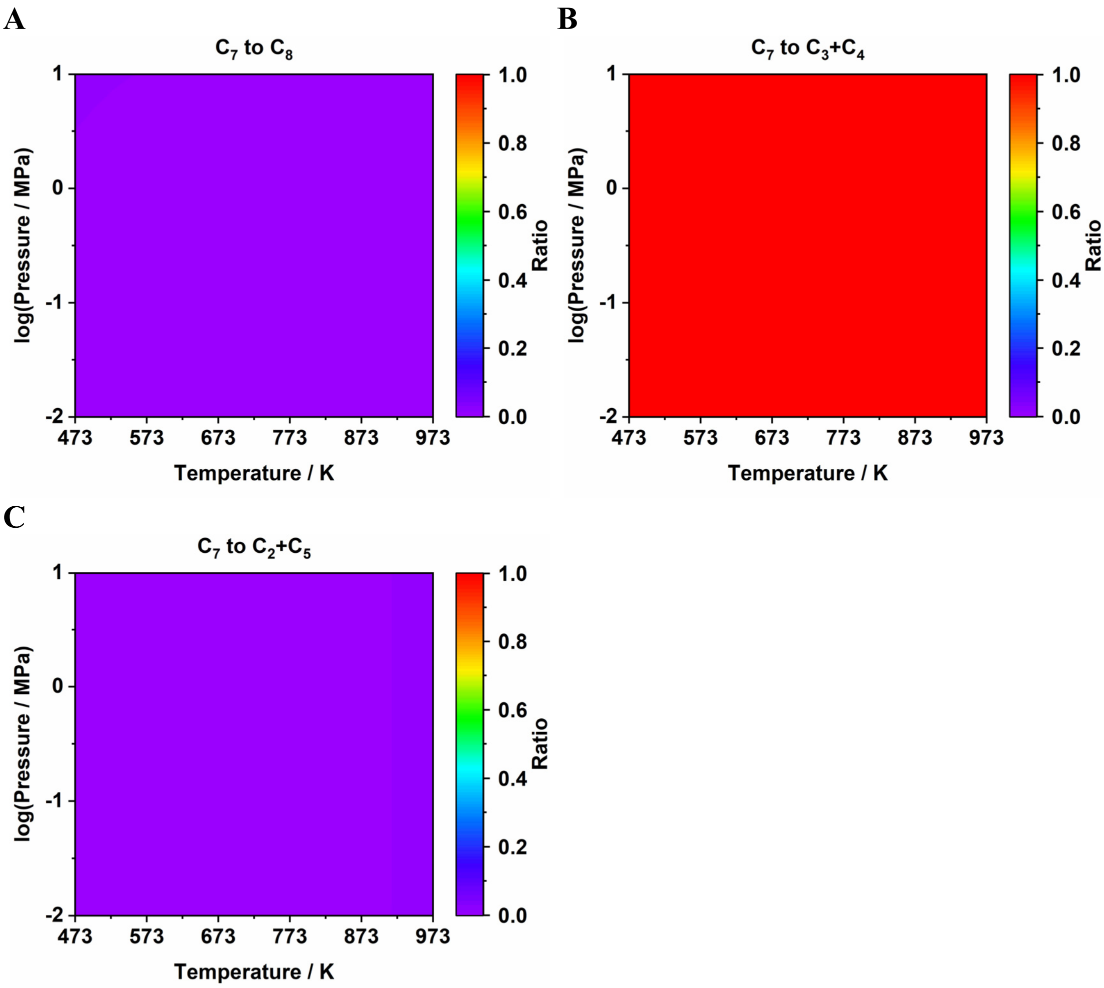

Figure S9. Evolution of C_7 methylation to C_8 **(A)** and C_7 cracking to C_3+C_4 **(B)** and C_2+C_5 **(C)** intermediates as a function of temperature and pressure in H-SAPO-34 for the conversion of ketene to olefins.

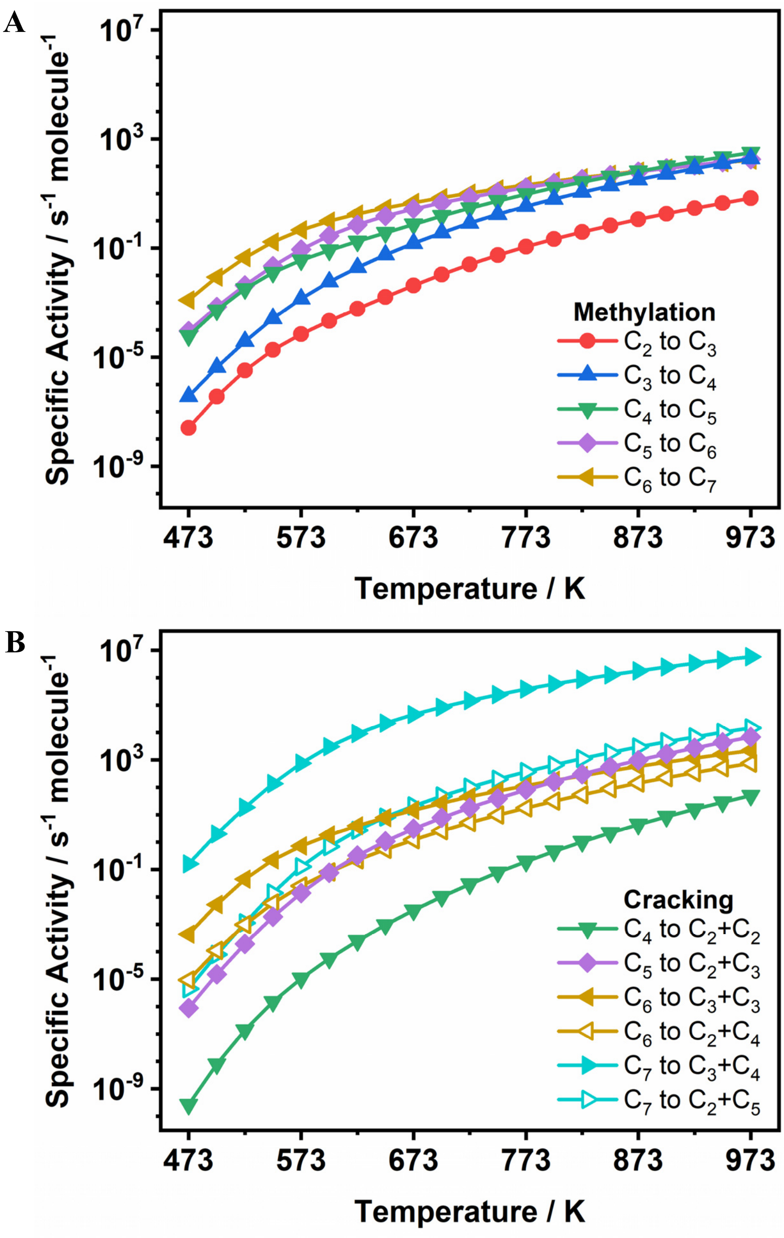

Figure S10. Simulated specific rates of methylation (**A**) and cracking (**B**) for each olefinic HCP as a function of temperature in H-SAPO-34 for the conversion of ketene to olefins at 0.1 MPa. The specific rate of each HCP is normalized to its amount.

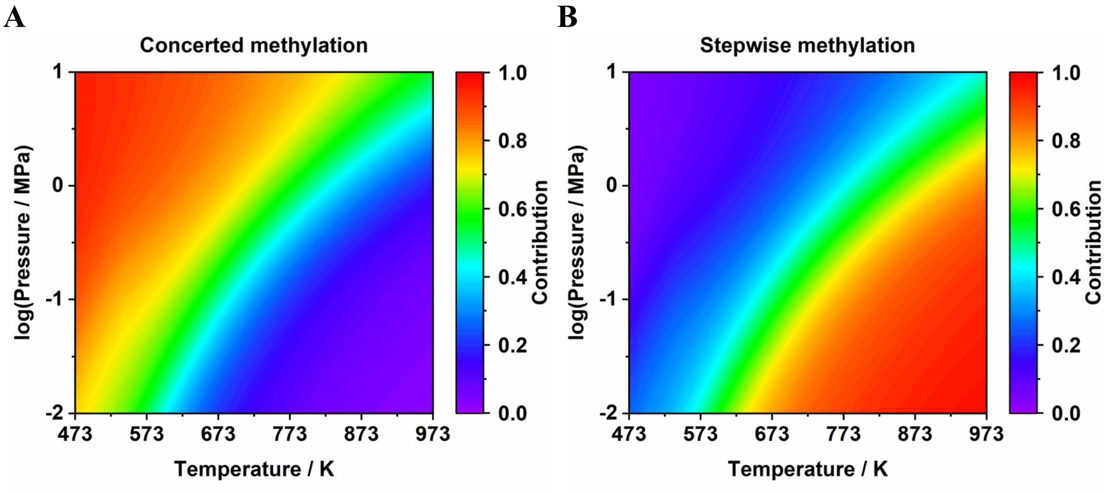

Figure S11. Relative contribution of the concerted (A) and stepwise (B) pathways to the methylation as a function of temperature and pressure in H-SAPO-34 for the conversion of ketene to olefins.

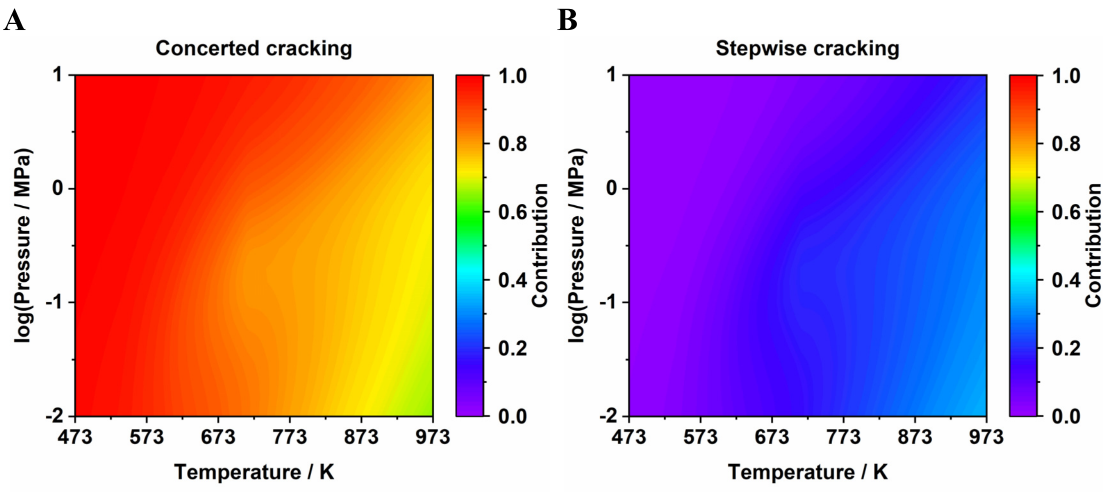

Figure S12. Relative contribution of the concerted (A) and stepwise (B) pathways to the cracking as a function of temperature and pressure in H-SAPO-34 for the conversion of ketene to olefins.

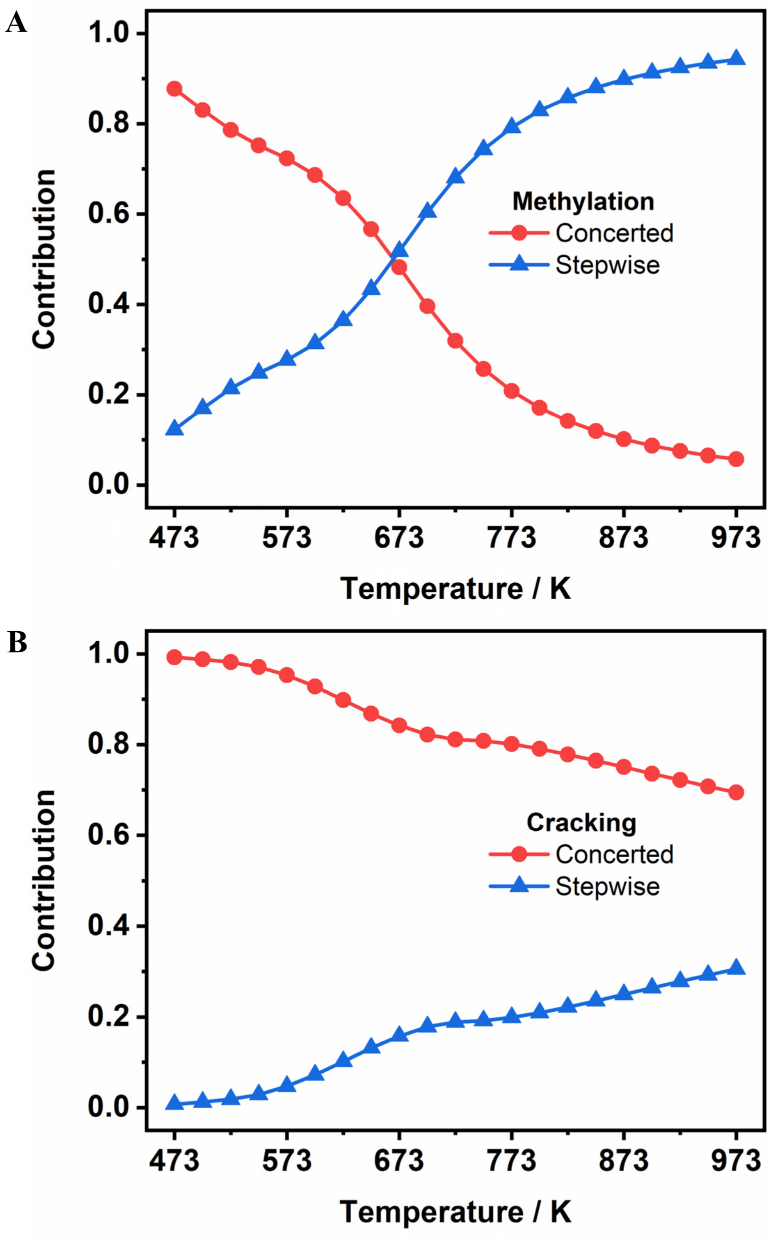

Figure S13. Relative contribution of possible pathways to the methylation **(A)** and cracking **(B)** as a function of temperature in H-SAPO-34 for the conversion of ketene to olefins at 0.1 MPa.

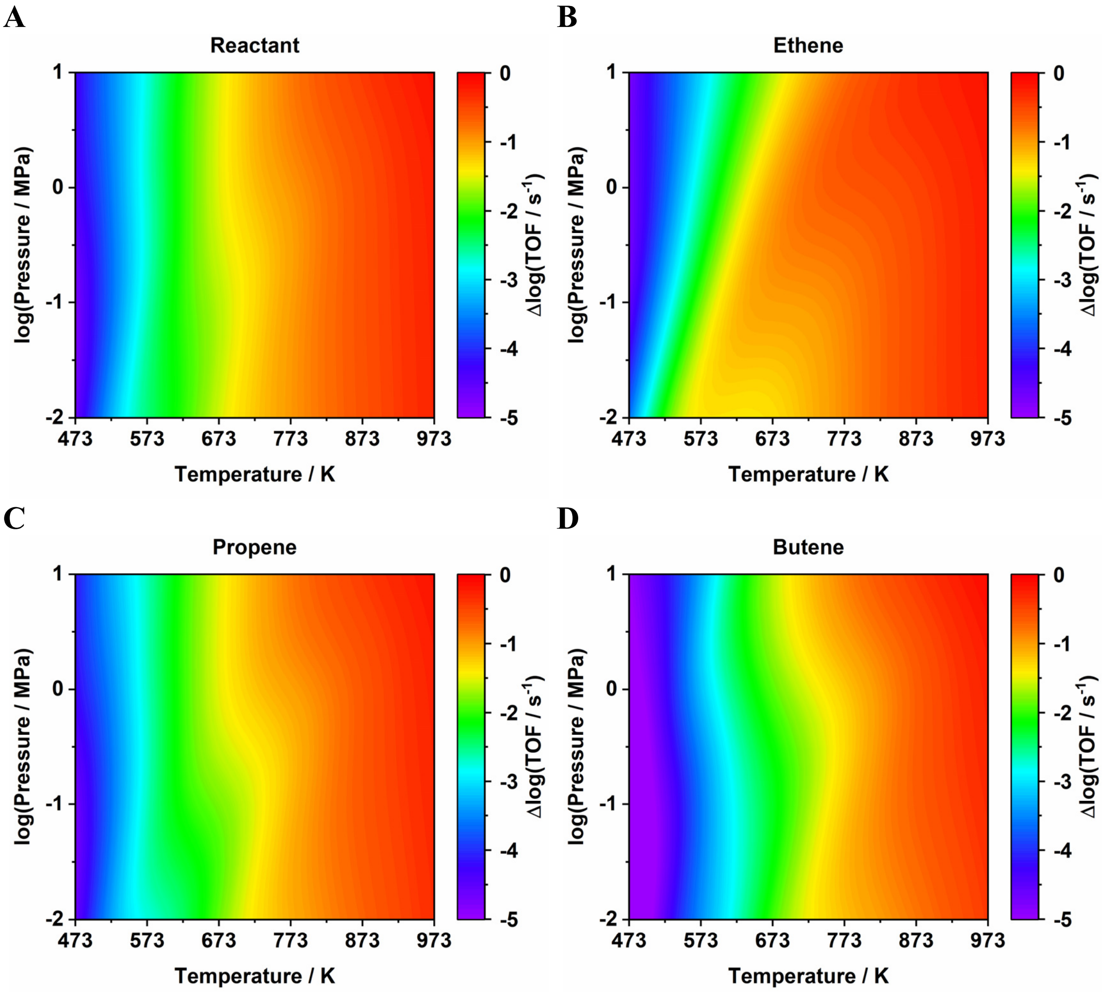

Figure S14. Rate differences in the conversion (**A**) and the formation of ethene (**B**), propene (**C**), and butene (**D**) of the ketene conversion to the methanol conversion as a function of temperature and pressure in H-SAPO-34. The rate difference is defined as log($TOF_{[ketene]}/TOF_{[methanol]}$). The methanol conversion activities were taken from [Ref. S1].

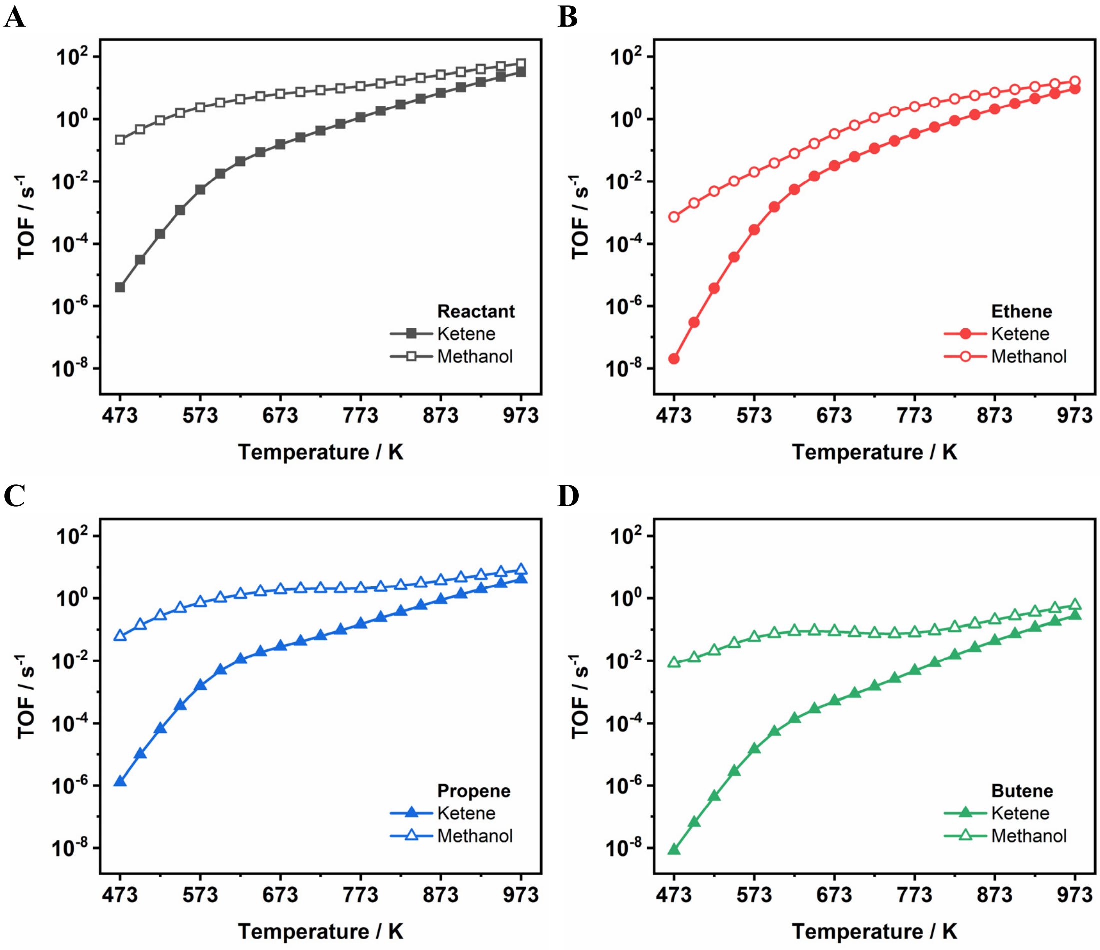

Figure S15. Conversion rates (**A**) and ethene (**B**), propene (**C**), and butene (**D**) formation rates of the ketene and methanol conversions as a function of temperature in H-SAPO-34 at 0.1 MPa. The methanol conversion activities were taken from [Ref. S1].

Effect of site ratio on simulated results

The ratio of HB to HP site affects the rates, the distribution of intermediates and the relative contribution of two methylation pathways, while exert slight effect on the selectivity, the cracking style and contribution of each pathway, and the origin of three olefins for the conversion of ketene to olefins (Figure X1−X3). At the conditions of 0.1 MPa & 673 K, the formation rates of each olefin product increase about two orders of magnitude when the ratio of HB:HP site increases from 1 to 1000, and the majorities of the retained olefins shift from C_2−C_4 to C_5−C_6 species (Figure X1). The increase of the contribution of the stepwise methylation (Figure X2) in HB site may accelerate the methylation activity of C_2−C_4 species. Thus, the conversion rate is improved by the introduction of additional acid sites.

The ratio of simulated T to HP site for the conversion of ketene to olefins is neglectable (Figure X4).

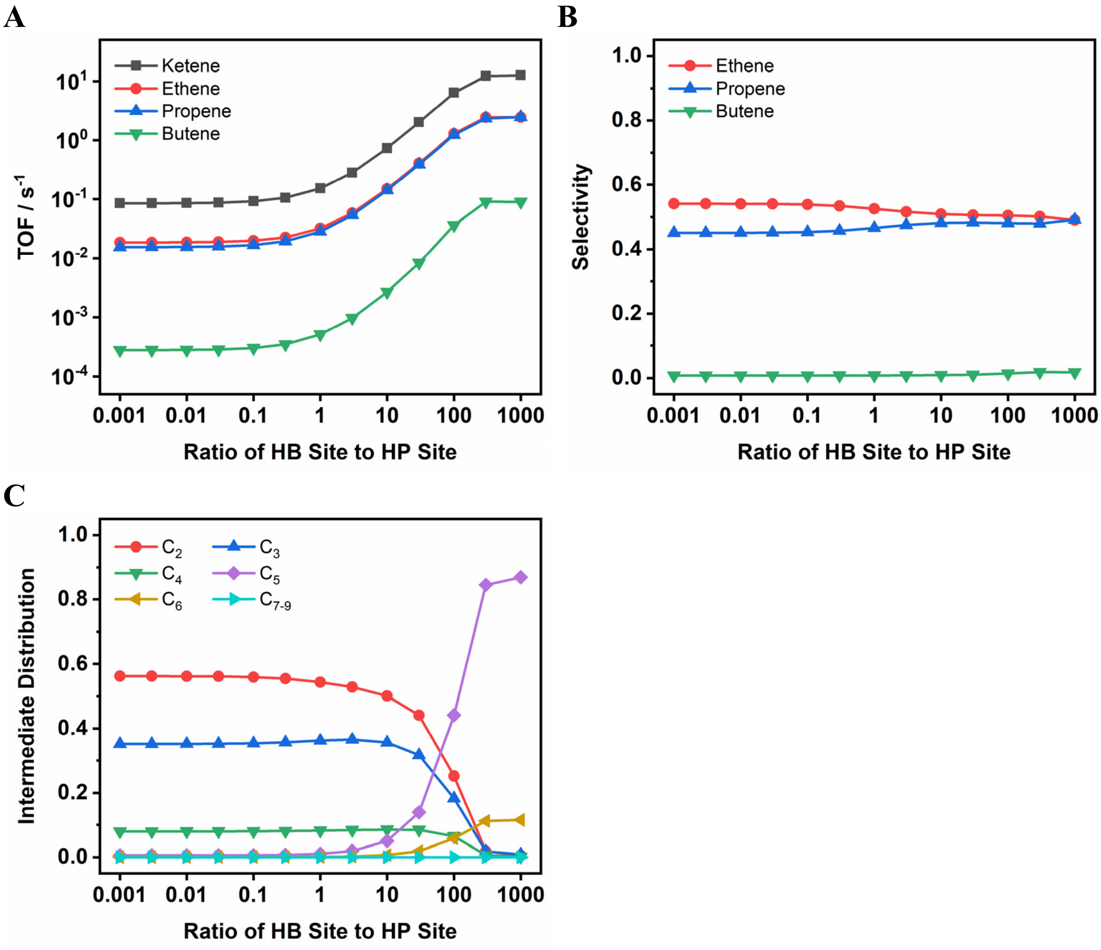

Figure X1. Activity **(A)**, selectivity **(B)**, and intermediate distribution **(C)** as a function of HB:HP site ratio in H-SAPO-34 for the conversion of ketene to olefins (Reaction conditions: 673 K, 0.1 MPa, CH_2CO:CO = 1:1, and HB:HP:T = 0.001−1000:1:1).

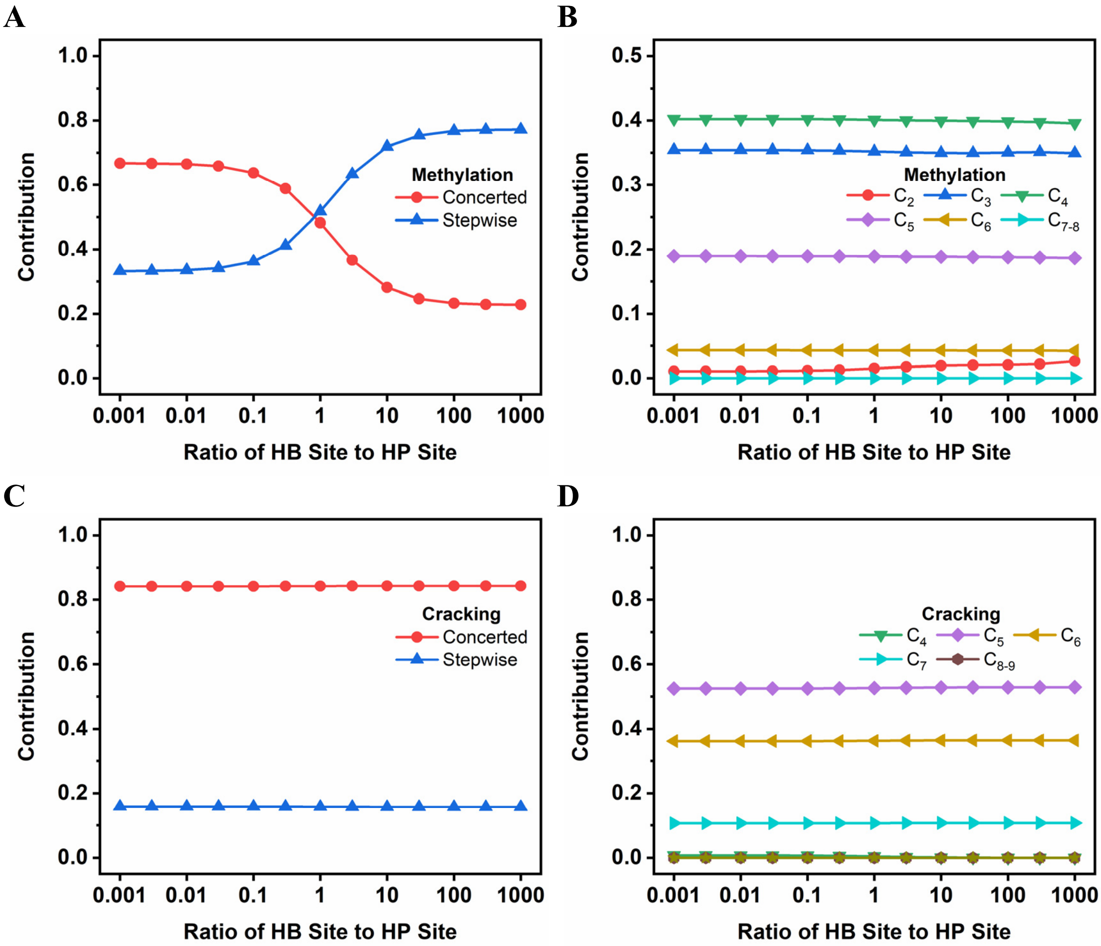

Figure X2. Relative contribution of possible methylation (**A**) and cracking (**C**) pathways, and evolution of intermediates (**B**, **D**) as a function of HB:HP site ratio in H-SAPO-34 for the conversion of ketene to olefins (Reaction conditions: 673 K, 0.1 MPa, CH_2CO:CO = 1:1, and HB:HP:T = 0.001−1000:1:1).

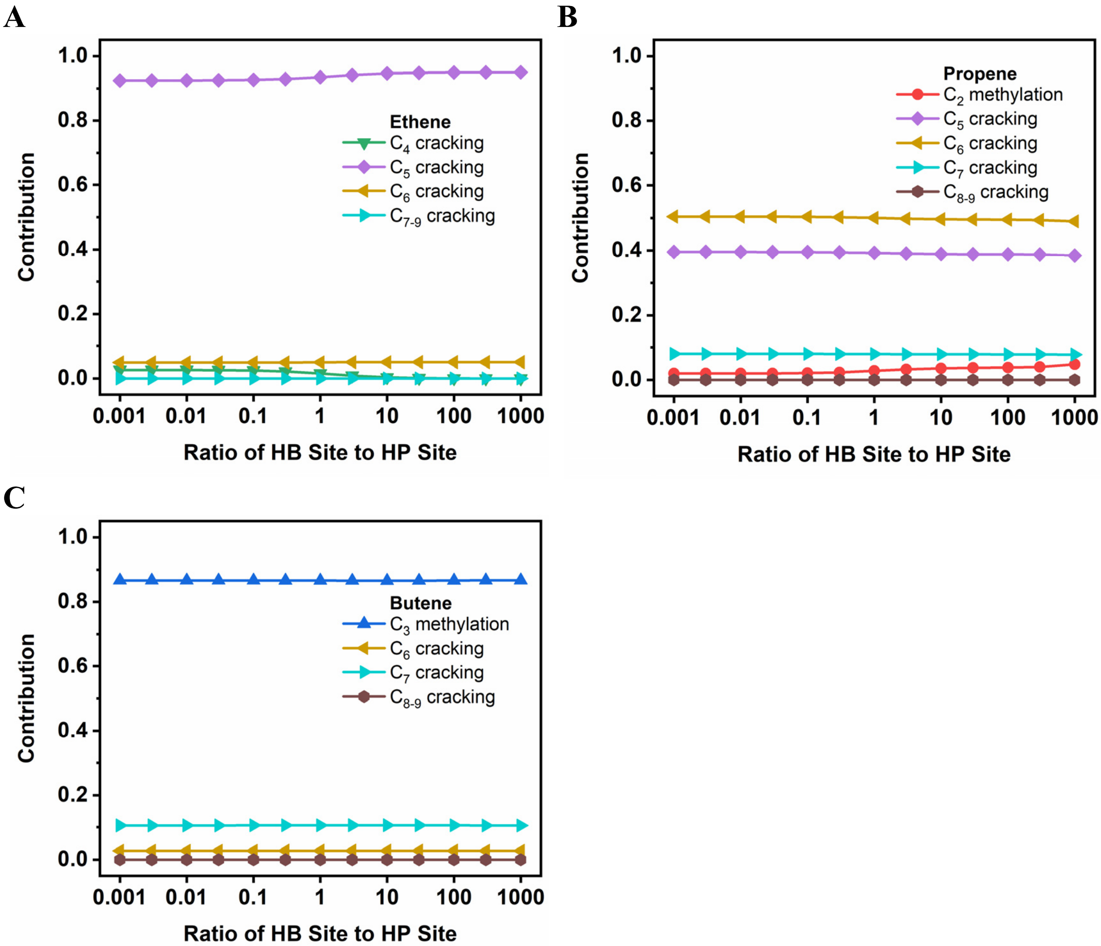

Figure X3. Origin of ethene **(A)**, propene **(B)**, and butene **(C)** as a function of HB:HP site ratio in H-SAPO-34 for the conversion of ketene to olefins (Reaction conditions: 673 K, 0.1 MPa, CH_2CO:CO = 1:1, and HB:HP:T = 0.001−1000:1:1).

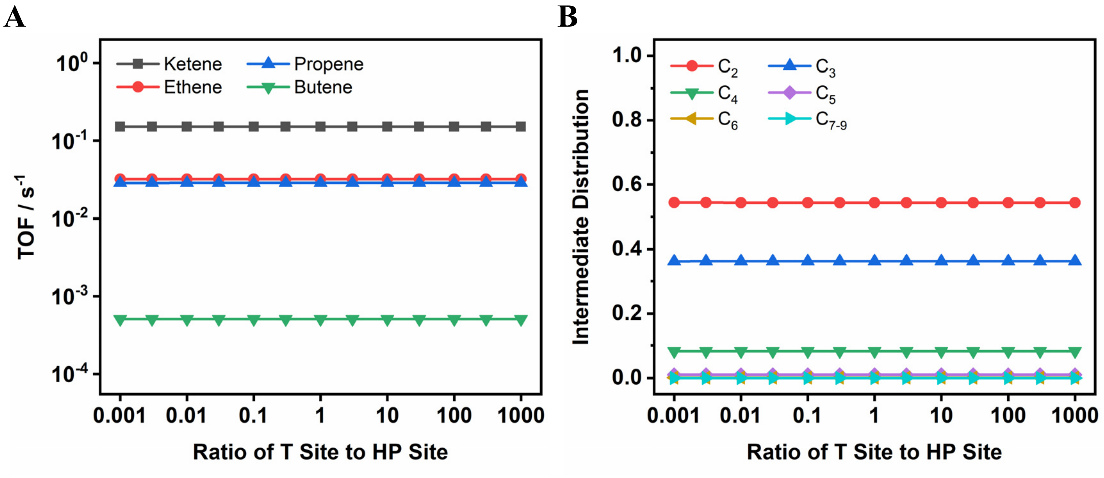

Figure X4. Activity **(A)** and intermediate distribution **(B)** as a function of T:HP site ratio in H-SAPO-34 for the conversion of ketene to olefins (Reaction conditions: 673 K, 0.1 MPa, CH_2CO:CO = 1:1, and T:HP:HB = 0.001−1000:1:1).

Reference

[S1] Ke, J.; Hu, W.-D.; Du, Y.-J.; Wang, Y.-D.; Wang, C.-M. Microkinetic simulations of methanol-to-olefin conversion in H-SAPO-34: Dynamic distribution and evolution of the hydrocarbon pool and implications for catalytic performance. *ACS Catalysis*, **2023,** *13*, 8642−8661.